

AMS-02: Cosmic electron and positron ($e^- + e^+$) spectrum up to 1 TeV

J. Bazo^{1,2,a} on behalf of the AMS-02 Collaboration

¹ INFN, Sezione di Perugia, 06123 Perugia, Italy

² INFN, Sezione di Tor Vergata, 00133 Roma, Italy

Abstract. The AMS-02 spectrometer, on the ISS since 2011, performs highly accurate measurements of cosmic rays up to the TeV region. We review the analysis of the cosmic ($e^+ + e^-$) flux in the energy range between 0.5 GeV and 1 TeV, based on 10.6 million ($e^+ + e^-$) events. The high statistics and detector energy resolution allow for a study of the spectral shape of unprecedented quality, thus improving our understanding of the production, acceleration and propagation of cosmic rays. The resulting energy spectrum does not show prominent features.

1. Introduction

A large experimental effort has been undertaken in the last 50 years by balloon, space born and ground based detectors in order to study the cosmic ray (CR) electron component in an extended energy range. Electrons can probe the origin and propagation of cosmic rays in the the local interstellar medium in a complementary way with respect to the hadronic CR component.

Production of CR that is solely due to super nova remnants (SNRs) is not enough to explain the observed spectral features of CR electrons under the standard propagation model. These features (e.g. the increase of the positron component in the positron fraction) could have different explanations, for example exotic sources (e.g. neutralino annihilation), or pulsar production. To understand the processes behind the observed spectral features high accuracy and high statistics measurements are needed.

The Alpha Magnetic Spectrometer (AMS) [1, 2] has precisely measured the positron fraction and the positron flux $\Phi(e^+)$ up to 500 GeV and the electron flux $\Phi(e^-)$ up to 700 GeV. They provide information on the combined flux $\Phi(e^+ + e^-)$ up to 500 GeV. In this proceeding we summarize the measurement of $\Phi(e^+ + e^-)$ up to 1 TeV [3] with reduced statistical and systematic errors.

2. The AMS-02 detector

AMS is a general purpose high-energy particle physics detector installed on the International Space Station (ISS) to conduct a long-duration (~ 20 -year) mission of fundamental physics research in space [4]. It consists of a tracker, a magnet, a time of flight (TOF), anti-coincidence counters, a ring imaging Cherenkov detector, an electromagnetic calorimeter (ECAL) and a transition radiation detector (TRD).

^a e-mail: JoseLuis.Bazo@pg.infn.it

The 9-layer double-sided silicon microstrip tracker determines the trajectory and absolute charge $|Z|$ of CR using multiple measurements of the coordinates and energy loss. Together with the 0.14 T permanent magnet, the tracker measures the particle rigidity.

The four TOF planes trigger the readout of all the detectors and measure the particle velocity and direction. The anti-coincidence counters inside the magnet bore are used to reject particles outside the geometric acceptance. The tracker, TOF, and TRD measure $|Z|$ independently. The curvature measured with the tracker and the magnet and the direction of the particle measured with the TOF give the sign of the charge.

The 3-dimensional imaging capability of the 17 radiation length ECAL allows for an accurate measurement of the $(e^+ + e^-)$ energy E scaled to the top of AMS and of the shower shape. An ECAL estimator, based on a boosted decision tree algorithm, is used to differentiate $(e^+ + e^-)$ from protons by exploiting their different shower shapes. To further differentiate between $(e^+ + e^-)$ and protons, signals from the 20 layers of proportional tubes in the TRD are combined into a TRD classifier formed from the product of the probabilities of the $(e^+ + e^-)$ hypothesis.

AMS operates continuously on the ISS and is monitored and controlled from the ground. The detector performance is steady over time. A Monte Carlo program based on the GEANT 4.9.4 package is used to simulate physics processes and detector signals.

3. Analysis

A major experimental advantage of the combined flux analysis compared to the measurement of the individual positron and electron fluxes, particularly at high energies, is that the selection does not depend on the charge sign. Another advantage is that it has a higher overall efficiency. Consequently, this measurement is extended to 1 TeV with less overall uncertainty over the entire energy range.

Data collected from May 19th, 2011 to November 26th, 2013 have been analyzed. The isotropic $(e^+ + e^-)$ flux measured in energy bins of width ΔE is given by:

$$\Phi(e^+ + e^-) = \frac{N(E)}{A_{\text{eff}}(E)\epsilon_{\text{trig}}(E)\epsilon_{\text{ECAL}}(E)T(E)\Delta E} \quad (1)$$

where N is the number of $(e^+ + e^-)$ events, A_{eff} is the effective detector acceptance, ϵ_{trig} is the trigger efficiency, ϵ_{ECAL} is the signal selection efficiency of the ECAL estimator and T is the exposure time.

Equation (1) is evaluated independently in 74 energy bins from 0.5 GeV to 1 TeV. The bin width is chosen to be at least twice the energy resolution. The bin-to-bin migration error is 1% at 1 GeV decreasing to 0.2% above 10 GeV. The absolute energy scale uncertainty is 2% in the test beam energy range (10–290 GeV). Below 10 GeV it increases to 5% at 0.5 GeV and above 290 GeV to 5% at 1 TeV.

The event selection is done requiring a downward-going relativistic particle which hits in at least 8 out of 20 TRD layers and a single track passing through the tracker and ECAL. Events with an energy deposition compatible with a minimum ionizing particle in the first 5 layers of ECAL are rejected. Events with $|Z| = 1$ are selected using dE/dx in the tracker and TRD. Primary particles (i.e. not from atmospheric origin) are selected with the geomagnetic cutoff discussed below.

TRD classifier reference spectra of the $(e^+ + e^-)$ signal and the proton background are used as templates. Templates are built from data using pure samples of e^- and protons and are evaluated separately in each bin. However since the signal templates show no energy dependence above ~ 10 GeV, all the e^- selected in the range 15.1–83.4 GeV are taken as a

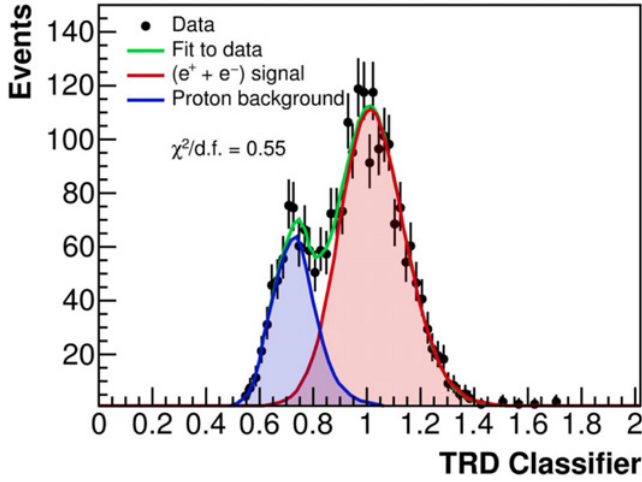


Figure 1. Result of the template fit in the 149–170 GeV energy bin showing the ($e^+ + e^-$) signal and proton background. The fit has a $\chi^2/\text{d.f.} = 0.55$ [3].

unique signal template. The sum of the signal and background templates is fit to the data by varying their normalizations. This gives the number of signal ($e^+ + e^-$) events N and the number of background events. Figure 1 shows the data, the fit and the signal and background templates for one example bin.

A total of 10.6×10^6 ($e^+ + e^-$) events have been identified with energies from 0.5 GeV to 1 TeV.

The effective detector acceptance is defined as:

$$A_{\text{eff}} = A_{\text{geom}} \epsilon_{\text{sel}} (1 + \delta) \quad (2)$$

where A_{geom} is the geometric acceptance, ϵ_{sel} is the event selection efficiency and δ is a data driven correction. The acceptance for a particle passing through the active volumes of the tracker, TRD, TOF, and ECAL is $A_{\text{geom}} \simeq 550 \text{ cm}^2 \text{ sr}$ and ϵ_{sel} has typical values of 90% at 10 GeV and 70% at 1 TeV. Both A_{geom} and ϵ_{sel} are evaluated from Monte Carlo simulation.

The small acceptance correction δ is obtained comparing data and simulation efficiencies for each selection cut. This correction is a smooth, slowly varying function of energy (-0.04 at 10 GeV and -0.03 at 1 TeV).

The trigger efficiency is determined from data. The DAQ is triggered by the coincidence of all four TOF planes. AMS also records unbiased triggers which require a coincidence of any three out of four TOF planes used to measure ϵ_{trig} . The trigger efficiency is 100% above 3 GeV decreasing to 75% at 1 GeV.

The ECAL estimator efficiency ϵ_{ECAL} is measured from data using negative rigidity samples and the selection cuts. Optimal ϵ_{ECAL} values range from 75% to 95% for different energy bins, depending on the number of signal and background events.

The orbital parameters and detector status are recorded every second of data-taking. Livetime-weighted seconds are added to obtain the exposure time in a given energy bin when the minimum bin energy exceeds 1.2 times the maximum Strömer cutoff for $|Z| = 1$ particles in the AMS geometric acceptance. The exposure time excludes time spent in the South Atlantic Anomaly, during TRD gas refills, and when the AMS z axis was more than 40° from the local zenith. For the energy bins above ~ 30 GeV, where the effect of the geomagnetic cutoff is negligible, the exposure time is 6.2×10^7 s, decreasing to 1.5×10^7 s at 5 GeV.

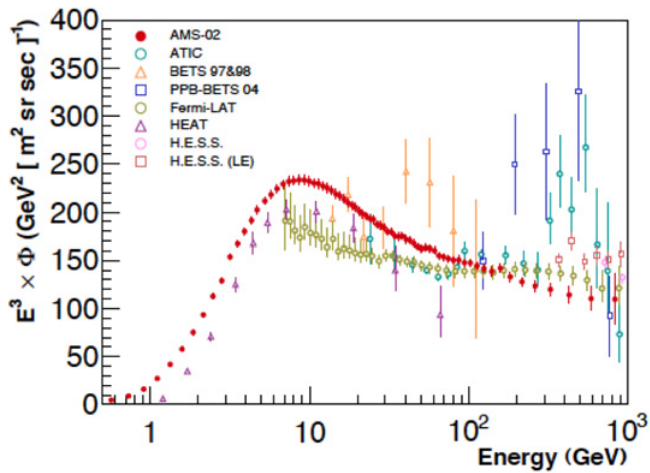


Figure 2. Electron plus positron flux $\Phi(e^+ + e^-)$ measured by AMS multiplied by \tilde{E}^3 versus energy. AMS total errors are the quadratic sum of the statistical and systematic errors [3]. Also shown are the results from earlier experiments [6–12].

3.1 Systematic errors

Systematic uncertainties come from the event selection, the acceptance and bin-to-bin migration discussed above.

The event selection systematic uncertainty, which includes the uncertainty from the construction of the templates, is evaluated from 2000 trials performed in each energy bin. Each trial consisted in reproducing the complete analysis. The trials were performed with different values of the ECAL estimator cut and different values of selection cuts used to construct the templates.

The number of signal events corrected by the ECAL estimator selection efficiency $N_E = N/\epsilon_{\text{ECAL}}$ is stable within the optimal range of ϵ_{ECAL} . The median value of the N_E distribution from the 2000 trials determines the flux. The RMS spread of the distribution provides an evaluation of the stability of the measurement. The difference between the width of this distribution in data and the expected statistical fluctuations gives the systematic uncertainty as $<1\%$ below ~ 200 GeV increasing to 4% in the 500–700 GeV bin. This is the main source of systematic uncertainty above ~ 500 GeV.

The acceptance systematic error is given by the uncertainty on δ . It is estimated from data to simulation comparisons. Above 3 GeV a systematic of 2% on $(1 + \delta)$ is obtained from the contributions of all cuts, increasing to 6% at 1 GeV. This is the major contribution to the systematic error below ~ 500 GeV. The acceptance systematic error includes a bin-to-bin correlation of 1.4% over the whole energy range.

4. Results

The measured $(e^+ + e^-)$ flux multiplied by \tilde{E}^3 [5] including its statistical and systematic errors is shown in Fig. 2 as a function of the energy at the top of the instrument together with previous measurements [6–12].

Below ~ 10 GeV solar modulation affects the behavior of $\Phi(e^+ + e^-)$. However, above 20 GeV these effects are negligible within the current experimental accuracy. The flux is smooth and shows no structures from 10 GeV to 1 TeV, revealing new information.

The flux cannot be described by a single power law ($\Phi \propto E^\gamma$) over the entire range. The lower energy limit above which a single power law (consistent spectral indices at the 90% C.L.) can describe the flux is estimated to be 30.2 GeV.

Fitting a single power law over the range 30.2 GeV to 1 TeV yields $\gamma = -3.170 \pm 0.008 \pm 0.008$ where the first error is the combined statistical and systematic uncertainty and the second error is due to the energy scale uncertainty.

5. Conclusions

As mentioned in [2], a single power law can describe the electron flux above 52.3 GeV and one with a different spectral index describes the positron flux above 27.2 GeV. However, the simultaneous single power law behavior of $\Phi(e^+)$, $\Phi(e^-)$, and $\Phi(e^+ + e^-)$ is unexpected.

An apparent tension between these results and some previous measurements can be avoided if the energy scale error from the different experiments is included in the figures. The energy scale error is smaller in the case of AMS-02.

The combined ($e^+ + e^-$) flux can be described by a minimal model where to the standard primary (e^-) particles accelerated by SNR and secondaries (e^+) produced in the interaction of nucleons with the ISM (both described by simple power laws), there is the need to add an additional production of primary e^-/e^+ by a common source (of diverse proposed origin, as pulsars or DM annihilation) parameterized by a power law with a cutoff energy.

This work is supported at the ASI Science Data Center (ASDC) under ASI-INFN agreements C/011/11/1 and No. 2014-037-R.0.

References

- [1] L. Accardo et al., Phys. Rev. Lett. **113** (2014) 121101
- [2] M. Aguilar et al., Phys. Rev. Lett. **113** (2014) 121102
- [3] M. Aguilar et al., Phys. Rev. Lett. **113** (2014) 221102
- [4] A. Kounine, Int. J. Mod. Phys. E **21** (2012) 1230005
- [5] G. D. Lafferty and T. R. Wyatt, Nucl. Instrum. Methods Phys. Res., Sect. A **355** (1995) 541 (1995). Eq. (6) was used with $\tilde{E} \equiv x_{lw}$
- [6] S. Torii et al., Astrophys. J. **559** (2001) 973
- [7] M. A. DuVernois et al., Astrophys. J. **559** (2001) 296
- [8] J. Chang et al., Nature (London) **456** (2008) 362
- [9] K. Yoshida et al., Adv. in Space Res. **42** (2008) 1670
- [10] F. Aharonian et al., Phys. Rev. Lett. **101** (2008) 261104
- [11] F. Aharonian et al., Astron. Astrophys. **508** (2009) 561
- [12] M. Ackermann et al., Phys. Rev. D **82** (2010) 092004